Journal of Machine Construction and Maintenance
QUARTERLY 4/2018(111)
ISSN 1232-9312
p. 33–40

Xiubing LIANG[1*], Yanhai CHENG[2], Xiaoqian CHENG[1], Yichao JIANG[2], Tadeusz KULIK[3], Jarosław FERENC[3]

[1] Academy of military science PLA China, National Innovation Institute of Defense Technology, Beijing, China
[2] School of Mechanical & Electrical Engineering, China University of Mining & Technology, Xuzhou, China
[3] Material Science and Engineering, Warsaw University of Technology, Poland
[*] Corresponding author: liangxb_d@163.com

THE EFFECT OF THE AMORPHOUS CONTENT OF LASER CLADDING Ni-Nb-Zr/CaF_2 ON MICROSTRUCTURE AND PROPERTIES

Key words: laser cladding; amorphous alloy; Ni-Nb-Zr; micro-hardness; corrosion resistance.

Abstract: Ni-Nb-Zr/CaF_2 amorphous coating was prepared on the surface of SA283GRA steel by adopting a high-power laser cladding system. The results show that the Ni-Nb-Zr/CaF_2 coating obtained by laser cladding has a good metallurgical bonding with the matrix of SA283GRA and the amorphous phase was obtained. The different amorphous content was obtained with varied laser power. With the increase of laser power, the dilution rate of the coating gradually increases, the amorphous phase content in the cladding coating decreased gradually, and crystallization near the substrate is significant in the laser coating. As the cladding coating is far from the substrate, the content of amorphous phase increases gradually, and the cladding coating has high thermal stability. The hardness of the Ni-Nb-Zr/CaF_2 amorphous coating prepared by a laser power of 4 kW is up to the highest value of 890 HV, which is about 4.7 times that of the base material. The electrochemical corrosion results show that the corrosion resistance of the amorphous layer is better than that of the substrate in NaCl solution with 3.5% corrosive medium. The Ni-Nb-Zr/CaF_2 laser coating has a relatively strong amorphous forming ability.

Powłoki Ni-Nb-Zr/CaF_2 z udziałem fazy amorficznej wytwarzane metodą natryskiwania laserowego – mikrostruktura i właściwości

Słowa kluczowe: natryskiwanie laserowe, stopy amorficzne, mikrotwardość, odporność korozyjna.

Streszczenie: Amorficzną powłokę Ni-Nb-Zr/CaF_2 otrzymano na powierzchni stali SA283GrA metodą natryskiwania laserowego, z wykorzystaniem laserów dużej mocy. Uzyskane wyniki badań wykazały, że powłoka Ni-Nb-Zr/CaF_2 charakteryzuje się dobrą przyczepnością do podłoża stalowego SA283GrA, a faza amorficzna jest otrzymywana w strefie przypowierzchniowej. Wykazano, że moc wyładowania laserowego istotnie wpływa na zawartość fazy amorficznej. Wraz ze wzrostem mocy lasera zawartość fazy amorficznej w strefie przypowierzchniowej zmniejsza się stopniowo, a stopień krystalizacji powłoki w pobliżu podłoża wzrasta. Zawartość fazy amorficznej zwiększa się gradientowo w funkcji odległości od podłoża. Największą twardość powłoki amorficznej Ni-Nb-Zr/CaF_2 890 HV uzyskano z wykorzystaniem lasera o mocy 4kW, tj. ≈4,7 razy większą w stosunku do materiału podłoża. Wyniki badań odporności korozyjnej metodą elektrochemiczną wykazały, że w roztworze NaCl z 3,5% odporność na korozję strefy przypowierzchniowej zawierającej fazę amorficzną jest większa niż odporność korozyjna podłoża. Wykazano również, że faza amorficzna Ni-Nb-Zr/CaF_2 ma stosunkowo dużą zdolność do formowania się w strefie przypowierzchniowej i charakteryzuje się dużą stabilnością temperaturową.

Introduction

In mines, oil, metallurgy, power generation, and other industries, serious problems such as wear and corrosion of equipment have caused early damage of equipment and wasted a large amount of resources. Surface engineering technology is an effective technology to improve surface properties. Among them, laser cladding is a surface engineering technology with a high power density and rapid cooling rate of substrate (up to 10^6 K/s) [1]. The application of laser cladding to deposited coatings with high hardness and corrosion resistance on the surface of damaged parts has become an important way to remanufacture the parts and improve their service life. Amorphous alloy has excellent physical, chemical, and mechanical properties, and it has become the focus of research in the field of material science. It is a new type of functional material with great potential and prospect. High performance amorphous coatings produced by the laser cladding technology on the surface of parts and components can obviously improve the comprehensive performance of the surface of parts. Ni based amorphous is a kind of high-quality cladding material suitable for laser cladding and remanufacturing. It has been developed rapidly in the field of laser cladding amorphous coating in recent years, which has been widely studied by scholars at home and abroad. Ni-Nb-Zr amorphous alloy is one of the Ni based amorphous alloys with strong amorphous formation ability, and the amorphous alloy formed by it has excellent physical and chemical properties, as has been verified by a large number of experiments [2-8]. But up to now, few publications have reported the preparation of Ni-Nb-Zr amorphous coatings by laser cladding method. In this paper, we used different experimental parameters to prepare Ni-Nb-Zr cladding coatings with different amorphous content. The microstructure, composition distribution, thermal stability, micro-hardness, and corrosion resistance of the prepared laser coating under different parameters was studied.

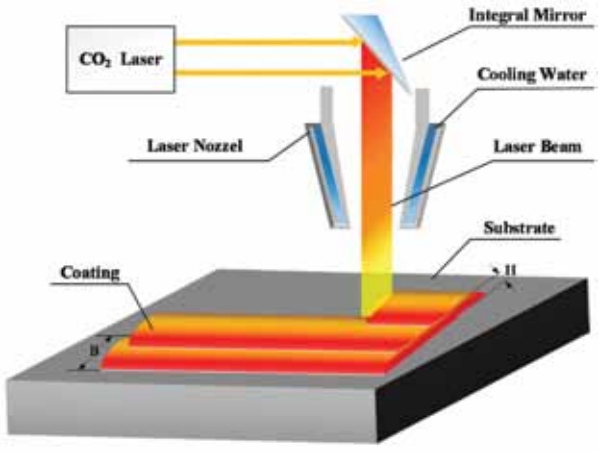

Fig. 1. Schematic illustration of laser melting

1. Experimental materials and method

The matrix material SA283GrA steel was chosen for the laser cladding. Before the experiment, the substrate was cut into 85 mm × 85 mm × 23 mm, and the surface of the substrate was mechanically polished and cleaned with an acetone solution in an ultrasonic cleaner. The particle size and purity of the cladding powder used in this experiment are shown in Table 1. The nominal composition of the cladding powder is $Ni_{62.5}Nb_{31.25}Zr_{6.25}$ (at %), and the mass fraction of each element is calculated to be $Ni_{51.37}Nb_{40.65}Zr_{7.98}$ (wt%) according to the relative atomic mass. In order to improve the moulding properties of the cladding powder, 5% CaF_2 powder [10–11] was added to form $(Ni_{51.37}Nb_{40.65}Zr_{7.98})_{95}(CaF_2)_5$ alloy powder.

Table 1. Composition of cladding powder

Element	Particle size (mesh)	Purity (%)	Atomic fraction (%)	Mass fraction (%)
Ni	-300	99.5	62.5	48.80
Nb	-325	99.95	31.25	38.62
Zr	-200	99.5	6.25	7.58
CaF_2	-300	98.5	-	5

A high-power semiconductor laser cladding system was used in the cladding process of the experiment. The output power of that system is 0~6 kW, the size of the laser beam is 2 × 18 mm, and the laser wave length is 900~1060 nm. The alloy powder was pre-placed on the substrate to form a powder bed before laser cladding. According to previous results of a relative experiment [9], the thickness of the cladding layer was set to be 1 mm, the overlap rate was 50%, and the scanning speed was 3 mm/s. The cladding parameters and energy density of each sample are shown in Table 2. The samples obtained were labelled Sample 1, Sample 2, Sample 3, and Sample 4, respectively. After completing the cladding process, surface dye detection was used to analyse the surface macroscopic cracks and pores of the laser coating, and the phase structure of the coating was analysed using a D8 ADVANCE X-ray diffractometer (XRD) with an accelerating voltage of 40 kV, a current of 30 mA, a Cu target, and a scanning speed of 0.02 sec/step. The metallographic structure of the coating was observed by a ZEISS optical microscope, and the microstructure of the coating was observed by a Quanta250 scanning electron microscope (SEM), and the attached EDS was used to perform line scan and surface scan in order to get the element distribution in the coating. The DSC curve of the laser coating was measured with a STA 449 F5 Jupiter simultaneous thermal analyser, and the thermal stability of the cladding layer was studied. The micro-hardness of the laser coating was measured by a Vickers tester (HVS-1000A). The corrosion resistance of the laser coating was tested by CHI660D electrochemical workstation.

Table 2. Energy density under different laser process

Sample No.	Laser power(kW)	Scanning speed(mm/s)	E (J/mm^2)
Sample 1	4	3	74
Sample 2	4.5	3	83
Sample 3	5	3	93
Sample 4	5.5	3	102

2. Results and discussion

2.1. Surface dye penetrant analysis and the effect of CaF_2

Figures 2 and 3 show the macroscopic appearance and the dye penetrant testing results of the laser coating. It can be seen from Fig.2 that the laser coating has a good forming quality and the surfaces of the layers are flat. We can also see from Fig. 3 that almost no cracks can be found in those samples except that there is a small amount of cracking found in Sample 2 and Sample 3. The good forming ability of cladding layers indicates that the addition of CaF_2 powder plays an important role in improving the forming quality of cladding layers. As a commonly used addition, CaF_2 has a wide range of applications in casting and welding. In the casting process, adding the proper amount of CaF_2 is beneficial to the melting of the metal. However, in the welding process, CaF_2 is added to the coating of the arc welding electrode, which can dehydrogenate and adjust the viscosity of the welding slag during the welding process. The addition of a small amount of CaF_2 to the Ni-based powder can significantly improve the process performance of the laser coating, and it can also significantly reduce the splash of powder during the cladding process. The surface of the Ni-based amorphous laser coating containing CaF_2 has no obvious defects such as pores and macro cracks, and the wettability of the coating and the substrate is obviously improved. This is mainly due to the fact that CaF_2 has a low melting point and density, and its compatibility with alloying element is poor during the melting of the powder, so the molten CaF_2 can easily float on the surface up in the molten pool and evaporates. The floatation of CaF_2 promotes the flow of the molten pool and makes the element distribution in the molten pool more uniform. The slag formed by CaF_2 floatation can form a protective layer on the surface of the molten pool, isolates the air, and reduces the influence of harmful gases on the laser coating. In addition, the surface tension of the molten pool can be reduced and the fluidity can be improved by the slag formed by floatation. Therefore, the addition of CaF_2 improves the forming quality of the laser coating obtained by the laser cladding method.

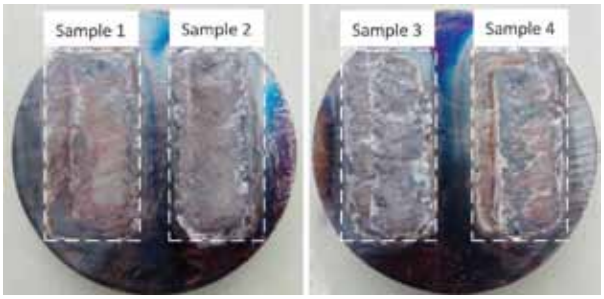

Fig. 2. Macroscopic appearance of Ni-Nb-Zr/CaF_2 laser coating (with CaF_2)

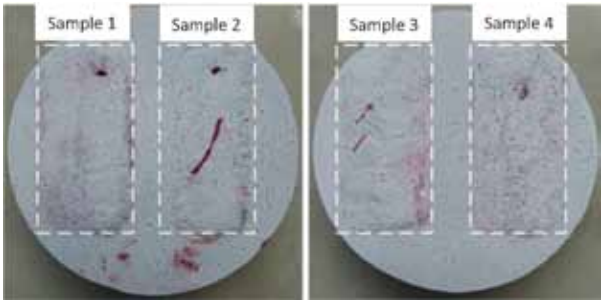

Fig. 3. Dye penetrant inspection results

2.2. XRD phase analysis

Figure 4 gives the X-ray diffraction pattern of the Ni-Nb-Zr/CaF_2 coating that was prepared under various laser power and is about 0.15 mm away from the surface. From Fig. 4, it can be seen that the coating obtained with the laser power of 4 kW formed on Sample 1 has a certain amount of amorphous phase and diffuse scattering peak at $40°<2\theta<50°$. For studying the effect of heat input on the amorphous content, the amorphous phase fraction of the coatings shown in the Fig. 5 was calculated by Pseudo-Voigt function fitting with Verdon [14]. With the increase of laser power, the X-ray diffraction pattern of coatings becomes obvious. It can be seen in Fig. 4 that the content of amorphous phase decreases when the heat input increases. Compared with Sample 1, as the laser coating obtained with laser power of 4.5 kW, the broadening diffusion peak of the amorphous phase of Sample 2 is smaller and the sharpness of diffraction peak intensity of the crystallized phase is obviously enhanced. The identified crystalline phase is iron and Fe7Ni3.

When further increasing the laser power, the content of the crystallized phase in the obtained coatings increased. In Fig. 5, the laser coating obtained with the laser power of 5 kW (Sample 3) and the laser coating obtained with the laser power of 5.5 kW l (Sample 4) have no broadening diffusion peak of the amorphous phase, while the diffraction peak of the crystalline phase increases. The reasons for such phenomenon can be summed up as follows: First, the laser cladding of amorphous alloys is formed under the condition of rapid cooling. The higher the laser power, the higher

the heat input into the coating and the matrix, the lower the corresponding cooling rate of the coating, which causes the cooling rate that could not meet the requirement of the amorphous phase formation. Second, with the increase of laser power, the heat input in the molten pool increases, the matrix material melts too much, and the dilution rate of elements like iron in the matrix increases, which causes the powder composition to deviate from the ideal composition range, and thus affects the formation of the amorphous phase.

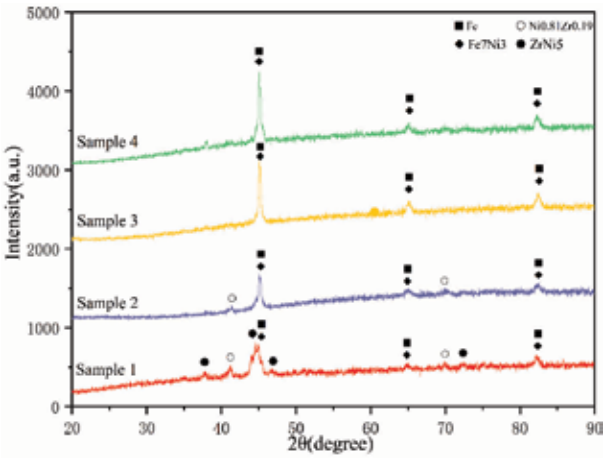

Fig. 4. X-ray diffraction patterns of Ni-Nb-Zr/CaF_2 laser coating prepared under different laser power

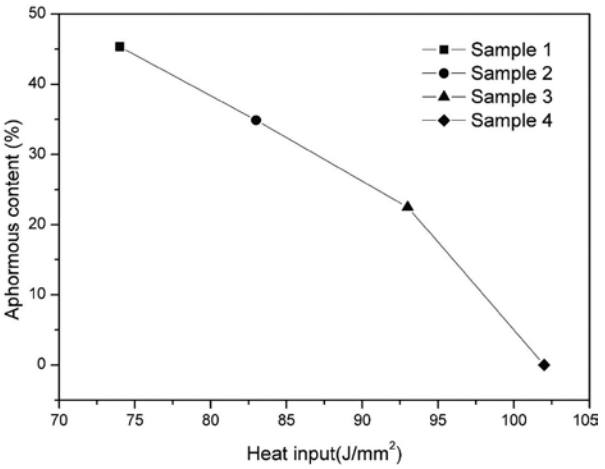

Fig. 5. The amorphous content under different heat input

2.3. Microstructural analysis

Figure 6 shows the microstructure of the laser coating obtained with the laser power of 4 kW (Sample 1) from the top to the bottom. It can be seen from the diagram that the microstructure of the laser coating changes regularly from the top to the bottom and consists of dendrites as amorphous phase and equiaxial crystal regions. The coating structure located in the top zone of the coating (Fig. 6a) consists of the equiaxial crystal, mainly because the surface of the laser coating is seriously affected by the surrounding environment during the cooling and solidification process. The directions of heat dissipation were varied; therefore, equiaxial crystals were formed on the top region of the laser coating and distributed along different directions. The central region of the layer is well protected during the deposition process, and the dilution effect of the matrix material in this region is small, which makes the alloy composition in the middle area of the coating close to the composition of the powder, and this ensures the strong amorphous forming ability, which can be observed as grey amorphous regions without morphology, as shown in Fig. 6b. Fig. 6c shows that the bottom structure of the coating has a dendrite structure perpendicular to the interface direction of the coating and the substrate. This is mainly due to the dilution of the coating material into the matrix material, which makes the alloy at the bottom of the layer have a crystalline structure. During the deposition process, the components from the substrate diffuse into the cladding material, and the result is that the coating near the substrate is similar in chemical composition and structure to the substrate material, and good cohesion is obtained between the cladding layer and the matrix. The molten metal is closely bonded to the substrate, together with good thermal conductivity of the area near the surface of the substrate, causing an epitaxial growth in the lower zone of the coating.

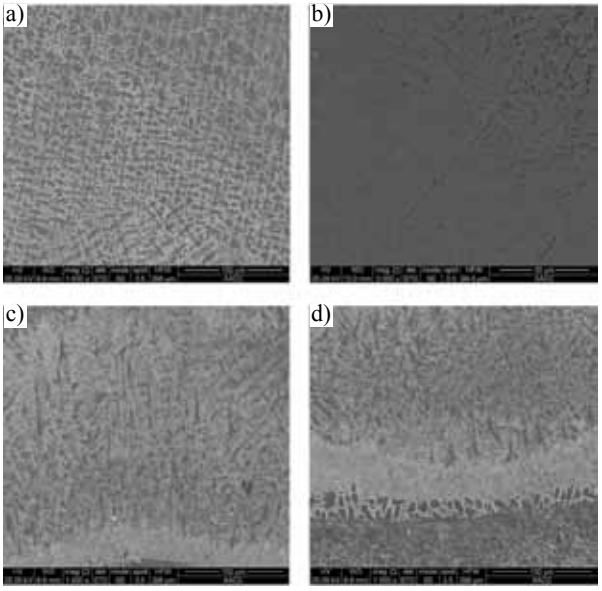

Fig. 6. Microstructure morphology of different regions of cladding layer (a) top (b) upper part (c) lower part (d) bottom

2.4. Composition analysis

To verify the composition change of the coatings obtained by the laser cladding method, the EDS line scanning analysis of the coating obtained with the laser

power of 4kW (Sample 1) on the vertical direction of the bonding line between the coating and the substrate is carried out. Fig. 7 indicates that, near the bond zone between the coating and the substrate material, the content of iron element shows a slow transition state. This is due to the diffusion of iron to the coating during the cladding process. With the increase of the distance from the surface of substrate, the content of iron in the cladding material becomes less. Accordingly, the content of nickel and niobium in the coating near the matrix is relatively small, which is also due to the dilution effect of the iron. In the middle region of the coating, the dilution effect of the matrix elements into the coating material decreases. Although the distribution of all elements in the cladding material are relatively even, the line scanning results still show the fluctuation of nickel and niobium composition, which indicates that the cladding process is a rapid heating and cooling process, and it is difficult to ensure the uniform diffusion of various elements in this process.

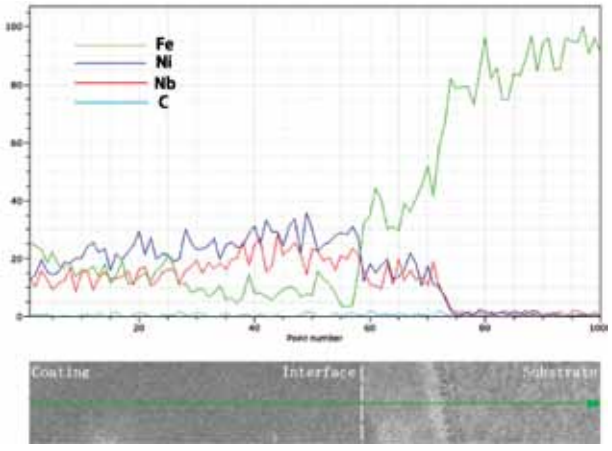

Fig. 7. Analysis of line scanning energy spectrum of cladding layer

Figure 8 shows the results of the morphology and element distribution of the coating obtained with the laser power of 4kW (Sample 1) near the middle region. Fig. 9(a) indicates that the obtained structure is not uniform. The columnar crystals appeared in the upper-right half, while the lower-left half has less crystals, and most of them are appeared in the form of a grey amorphous phase. The distribution of elements is further shown in Figs. 9b,c,d,e, and f. It can be seen that the grey zone of the amorphous phase contains a greater amount of nickel. The distribution of iron, niobium, and zirconium is regular.

2.5. Thermal Stability Analysis

Figure 9 shows the differential thermal analysis results at a constant heating rate of 20 $K \cdot min^{-1}$ for the laser coatings obtained by the laser cladding method

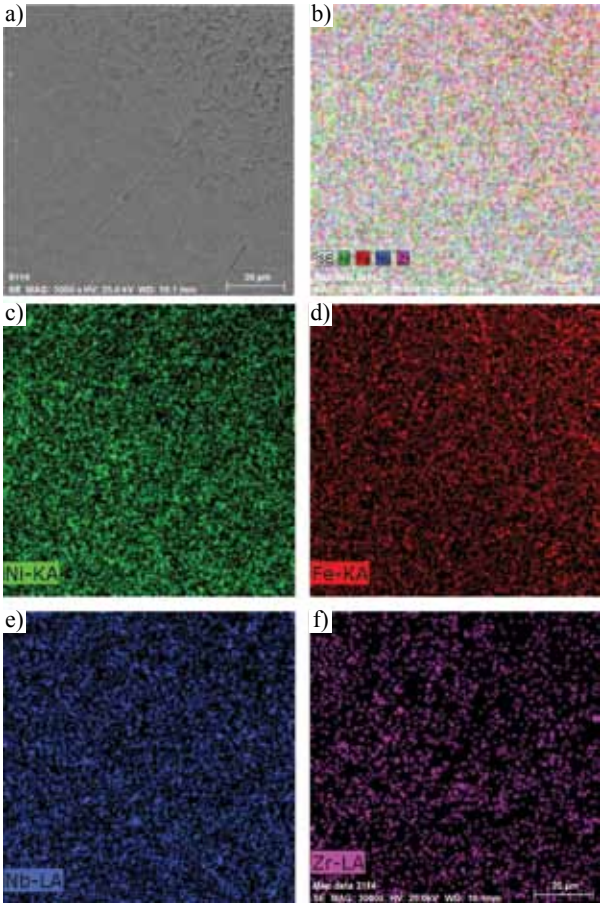

Fig. 8. The view of morphology (a) and surface istribution of chemical element (b,c,d,e,f) of the coating obtained with the laser power of 4kW (sample 1)

with different laser power. Fig. 9 indicates that Sample 1 prepared at a laser power of 4 $K \cdot min^{-1}$ has an exothermic peak, which indicates that there is a precipitation of a crystallized phase during the heating process, while there is no exothermal peak in the coatings of Samples 2, 3, and 4 prepared at relatively high laser power. This further shows that the content of the amorphous phase in Sample 1 is higher when compared to the remaining samples. The tangent method was further applied in order to obtain two important parameters to characterize the thermal stability of the coating: the glass transition temperature T_g and the crystallization temperature T_x. The glass transition temperature Tg of the coating obtained for Sample 1 was 536°C, and the crystallization temperature Tx was 618°C, indicating that the crystalline transformation will not occur when the lining layer will operate below 618°C. The achieved results also indicate that the coating obtained with the laser power of 4kW has relatively high thermal stability. In addition, the undercooled liquid region width ΔT_x was also an important parameter to characterize the glass forming ability of amorphous alloys [12–13]. The undercooled liquid region width ΔT_x of the cladding layer of Sample 1 was 82°C. Compared with the reported

[7] thermodynamic parameters of several Ni-Nb-Zr amorphous alloys, the Ni-Nb-Zr/CaF_2 laser coating prepared in this experiment has a relatively wide super cooled liquid region, indicating that the laser coating has a relatively strong amorphous forming ability.

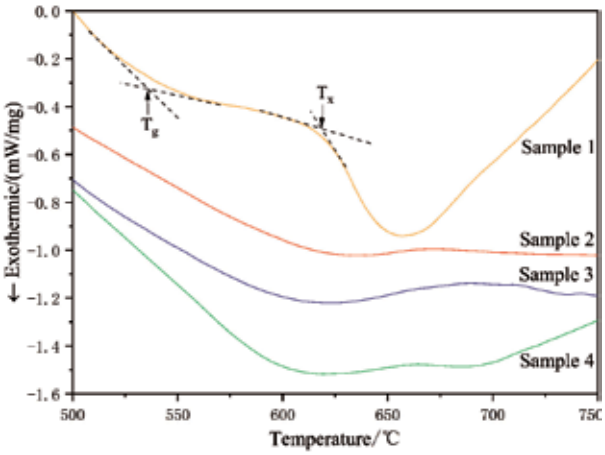

Fig. 9. DSC curve of the cladding layer at 20°C/min heating rate

2.6. Micro-hardness Analysis

Figure 10 shows the dependence of Vickers hardness of Samples 1, 2, 3, 4 as a function of distance from the surface. It also reveals that the width of heat affected zone is about 0.4 mm and the micro-hardness gradually decreases with the increase of the distance from interface. The micro-hardness of the heat affected zone ranges from 200 to 500HV.

Figure 10 shows that the micro-hardness of coating ranges from 450 to 890HV. The coating obtained with the laser power of 4kW (Sample 1) has the highest hardness, reaching 890.12 HV. When the laser power is increased to 4.5 kW, the highest hardness value of the coating reduces to 604.92 HV, which is approximately 3.2 times of the substrate material. As the laser power continues to increase, the hardness of the coating continues to decrease. When the laser power rises to 5 kW, the micro-hardness of the coating basically stabilizes and the maximum micro-hardness values of Samples 3 and 4 are 513.55 HV and 492.38 HV, respectively, about 2.6 times that of the substrate.

Moreover, the hardness distribution inside the coating also shows that the hardness value in the middle of the coating is the highest. This is because large amounts of crystalline phases are formed at the top of the layers, while the amounts of the crystalline phase decreases and the amounts of amorphous phase increase at the centre and bottom of the layers. As a result, the micro-hardness at the centre of the coating is relatively higher. This is also due to the fact that the middle portion of the coating maintains at a reasonable composition range, and the elements are evenly distributed, and there is a generation of an amorphous phase, as a result of that, a higher hardness is exhibited. Therefore, as the laser power increases, the amorphous content reduces and the hardness of the coating continuously decreases. Increasing amorphous content is beneficial to increase the hardness of the coating. Sample 1 has the largest amorphous content; therefore, the hardness is also the highest.

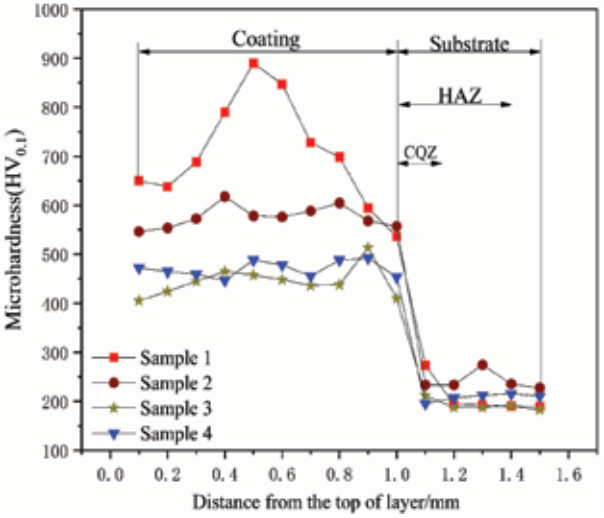

Fig. 10. Micro-hardness distribution of coating under different laser power

2.7. Corrosion Resistance Analysis

Figure 11 shows the Tafel polarization curves of the coating prepared under different laser cladding parameters. Table 3 shows the corrosion potential E_{corr} of the coating and the SA283GRA steel substrate and the corrosion current density $i_{corr.}$ Figure 11 and Table 3 obviously show that the self-corrosion potential of the cladding layer is higher than the self-corrosion potential of the base material, and the self-corrosion current density of the coating is lower than the self-corrosion current density of the base material. With the increase of laser power, amorphous content reduces, the corrosion potential of the coating gradually decreases, and the self-corrosion current density gradually increases. It was demonstrated that the Ni-based amorphous alloy coating prepared by laser cladding significantly improved the corrosion resistance of the SA283GRA steel substrate. The larger the amorphous content, the stronger the corrosion resistance of the prepared coating. In addition, the passivation plateau is formed after the coating entering the anodic polarization region, and the passivation regions of the amorphous coating prepared under different laser power are different. This is because the Nb and Zr elements present in the alloying elements of the coating are prone to passivation, and the surface of the coating rapidly forms a passivation film after entering the anodic polarization region, thereby

protecting the surface of the coating. As the potential continues to increase during the etching process, the passivation film on the surface of the coating is broken down and the corrosion process continues. It is also seen that the larger the amorphous content and the wider the passivation area, the more difficult the passivation film on the surface of the cladding layer is to be activated by breakdown, which indicates that the corrosion resistance of the coating is better.

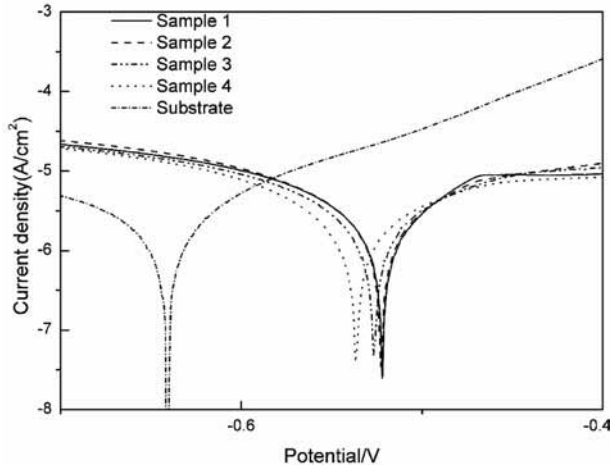

Fig. 11. Polarization curves of coating and substrate in 3.5%NaCl solution

Table 3. Corrosion potential (E_{corr}) and corrosion current (i_{corr}) of coating and substrate in 3.5% NaCl solution

Sample No.	E_{corr}(V)	i_{corr} (A/cm^2)
Sample 1	-0.517	3.245×10^{-6}
Sample 2	-0.522	3.307×10^{-6}
Sample 3	-0.527	3.380×10^{-6}
Sample 4	-0.529	3.534×10^{-6}
Substrate	-0.641	4.013×10^{-6}

Conclusions

(1) There is amorphous phase formed in the Ni-Nb-Zr/CaF_2 coating prepared by laser cladding. The amorphous content in the coating prepared at different laser power is different. The content of the amorphous phase changes as a function of the distance from the surface. The change in the laser power affects the cooling rate and the intensity of the diffusion of the substrate components to the coating material and, as a result, the intensity of the formation of the amorphous phase in the coating.

(2) The coating and the substrate show good metallurgical bonding. The microstructure of the coating from the bonding zone to the top of the coating is a planar, dendritic, and amorphous microstructure. With the continuing increase of laser power, the grains become more and more coarse.

(3) The Ni-Nb-Zr/CaF_2 coating prepared by laser cladding has higher thermal stability, which obviously improves the micro-hardness and corrosion resistance of the SA283GRA steel substrate. With the increase of laser power, the micro-hardness and the corrosion resistance of the Ni-Nb-Zr/CaF_2 coatings obtained by the laser cladding method gradually decreases as well.

Acknowledgements

This work is supported by the National Natural Science Foundation Projects [NO.51676205], National Key R&D Program [SQ2018YFC190082].

References

1. Barekat M., Shoja Razavi R., Ghasemi A.: Nd: YAG laser cladding of Co-Cr-Mo alloy on γ-TiAl substrate. *Optics & Laser Technology*, 2016, 80, pp. 145–152.
2. Li D., Zhu Z., Zhang H., Wang A., Hu Z.: The influence of Zr substitution for Nb on the corrosion behaviors of the Ni-Nb-Zr bulk metallic glasses. *Science China Physics, Mechanics and Astronomy*, 2012, 55(12), pp. 2362–2366.
3. Zhu Z.W., Zhang H.F., Ding B.Z., Hu Z.Q.: Synthesis and properties of bulk metallic glasses in the ternary Ni-Nb-Zr alloy system. *Materials Science and Engineering: A*, 2008, 492(1–2), pp. 221–229.
4. Hu H.T., Chen L.Y., Wang X.D., Cao Q.P., Jiang J.Z.: Formation of Ni-Nb-Zr-X (X=Ti, Ta, Fe, Cu, Co) bulk metallic glasses. *Journal of Alloys and Compounds*, 2008, 460(1–2), pp. 714–718.
5. Santos F.S., Kimimami C.S., Bolfarini C., de Oliveira M.F., Botta W.J.: Evaluation of glass forming ability in the Ni-Nb-Zr alloy system by the topological instability (λ) criterion. *Journal of Alloys and Compounds*, 2010, 495(2), pp. 313–315.
6. Qiang J.B., Zhang W., Inoue A.: Effects of Al and Ti additions on the thermal stability, glass-forming ability and mechanical properties of $Ni_{60}Nb_{20}Zr_{20}$ glassy alloy. *Materials Science and Engineering: B*, 2008, 148(1–3), pp. 114–118.
7. Chen L.Y., Hu H.T., Zhang G.Q., Jiang J.Z.: Catching the Ni-based ternary metallic glasses with critical diameter up to 3mm in Ni-Nb-Zr system. *Journal of Alloys and Compounds*, 2007, 443(1–2), pp. 109–113.
8. Xia L., Li W.H., Fang S.S., Wei B.C., Dong Y.D.: Binary Ni-Nb Bulk Metallic Glasses. *Journal of Applied Physics*, 2006, 99(2), 026103.

9. Cheng Y.H., Cui R., Wang H.Z., Han Z.T.: Effect of processing parameters of laser on microstructure and properties of cladding 42CrMo steel. *The International Journal of Advanced Manufacturing Technology*, 2018, 96(5–8), pp. 1715–1724.
10. Li R., Li Z., Zhu Y., Qi K.: Structure and corrosion resistance properties of Ni–Fe–B–Si–Nb amorphous composite coatings fabricated by laser processing. *Journal of Alloys & Compounds*, 2013, 580(32), pp. 327–331.
11. Wu X., Xu B., Hong Y.: Synthesis of thick Ni66Cr5Mo4Zr6P15B4 amorphous alloy coating and large glass-forming ability by laser cladding. *Materials Letters*, 2002, 56(5), pp. 838–841.
12. Inoue A., Zhang T., Masumoto T.: Glass-forming ability of alloys. *Journal of Non-Crystalline Solids*, 1993, 156, pp. 473–480.
13. Lu Z.P., Liu C.T.: A new glass-forming ability criterion for bulk metallic glasses. *Acta Materialia*, 2002, 50(13), pp. 3501–3512.
14. Verdon C., Karimi A., Martin J.L.: A study of high velocity oxy-fuel thermally sprayed tungsten carbide based coatings. Part 1: Microstructures. *Materials Science & Engineering A*, 1998, 246(1–2), pp. 11–24.